

Experimental measurements of multiple stable trapped domain wall states induced in nanofabricated elements

D. Lacour, J. A. Katine,* L. Folks, T. Block, J. R. Childress, M. J. Carey, and B. A. Gurney

Hitachi San Jose Research Center, 650 Harry Rd, San Jose CA 95120, USA.

(Dated: May 1, 2019)

Abstract

The presence of a domain wall trapped by a sub-micron notch is probed in two ways: through electronic transport measurements and by Magnetic Force Microscopy (MFM). We observe complex magnetic features which are consistent with numerical simulations predicting the existence of multiple magnetic configurations stabilized by the notch structure.

PACS numbers: 75.60.Ch, 68.37.Rt

arXiv:cond-mat/0306486v1 [cond-mat.mtrl-sci] 18 Jun 2003

*Electronic address: jordan.katine@hgst.com

Domain walls (DW) play a critical role in much of the current research involving spin-dependent electronic devices[1, 2, 3, 4, 5, 6]. In the case of a highly constrained DW, extremely large magnetoresistance ratios have been reported[1, 2]. Logic gates based on domain wall motion are being studied[3]. Recently, the movement of trapped DWs via the spin-transfer torque has been experimentally demonstrated in thin films[4, 5, 6]. Although the DW characteristics are key parameters in the aforementioned experiments, only a few theoretical[7, 8, 9] and experimental studies[10, 11] have been devoted to trapped DWs.

In this letter we present an experimental study of trapped DWs. Using a device geometry previously proposed by Ono, et al.[11] and subsequently employed by Grollier, et al.[5], we demonstrate that multiple stable locations exist for the trapped DW in such devices.

I. SAMPLE PREPARATION AND ELECTRICAL CHARACTERIZATION

Exchange biased spin-valve films consisting of Ta(3)/ NiFe(1.5)/ IrMn(5)/ CoFe(2.5)/ Cu(3)/ CoFe(4)/ NiFe(15)/ Ta(2.5) (thicknesses in nm) were sputtered onto a Si substrate. To fabricate the devices, we used a combination of e-beam lithography and reactive ion etching to produce a thin carbon hardmask. This mask protected the devices during the Ar ion milling used to etch the spin valve film. A second e-beam step was used to pattern thick Ta/Au leads allowing 4-probe device resistance measurements to be made. The left side of Fig. 1(a) is a schematic plane view of the device. There are two important features: a 50 μm square nucleation pad and a long (100 μm), narrow (0.5 μm) propagation line. The four gold leads (I+, V+, I- and V-) for measuring the propagation line resistance are also shown. A rectangular notch is positioned one-third of the way along the propagation line (see Fig.1(a) right). Different notch geometries have been fabricated, varying the notch width (W) from 500 nm to 50 nm.

Typical curves of the propagation line resistance as a function of the applied field (H_{app}) are shown in Fig.1(b). The resistance measurements were performed at room temperature using a standard 4-probe technique. The GMR signal is recorded during two different field loops. The first, corresponding to the ($-\blacktriangle-$) curve, is a minor loop during which the magnetization of the CoFe/NiFe bilayer (called free layer in the following) is completely reversed. The minimum and maximum states of resistance correspond respectively to the parallel and antiparallel alignment of the spin-valve magnetizations. Intermediate plateaus

at values corresponding to either 1/3 or 2/3 of the total resistance variation are present during the switching of the free layer magnetization. These plateaus indicate the existence of a magnetic configuration in which a DW present in the free layer is trapped at the notch[11]. In order to check the stability of this configuration at remanence, the propagation line resistance has been recorded during a second field loop: the $(-o-)$ curve in Fig. 1(b). After preparing the sample in a magnetic state where a DW is trapped in the notch, H_{app} is reversed. Note that the resistance remains at an intermediate level for $-20 \text{ Oe} < H_{app} < +3 \text{ Oe}$. So in this field range the DW stays trapped by the notch. To further investigate this specific magnetic configuration, MFM measurements have been performed.

II. RESULTS AND DISCUSSION

Using a commercial Digital Instruments scanning probe microscope equipped with a standard MESP tip, both topographic and MFM measurements were performed at room temperature. No external magnetic field was applied during the MFM scans, and the tip-sample separation was 18 nm. The topographic images for four different notch shapes ($W=500, 200, 100$ and 50 nm) are denoted “Topo.” in Fig. 2. The depth of the notch is 150 nm for all widths except for samples with $W=50$ nm where proximity effects in the negative e-beam resist made the notch depth 110 nm. With the electrical characterization technique previously described, we have been able to prepare the free layer of our samples in two different magnetic states at remanence named A and B in the following (see the resistance levels denoted A and B in Fig. 1(b)). The state A is characterized by the presence of a DW trapped by the notch. Conversely, no DW is present in the state B. The MFM scans obtained in the states A and B, for samples with $W=500, 200, 100$ and 50 nm, correspond respectively to the pictures labelled MFMA and MFMB in Fig. 2. Independent of the notch geometry, dark shapes (resembling a bat) centered on the notch are present on the MFMA pictures, while two black and white areas surrounding the notch are observable in the MFMB pictures.

The contrast of MFMB images have been reproduced well using the micromagnetic model OOMMF[12] (not shown here). Using the same model, the micromagnetic configuration and resulting MFM image at remanence has also been computed in the case of a trapped DW (state B) for different reverse fields values. Figure 3 shows the results of these simulations.

The absolute value of the reverse field is increased in 20 Oe increments, starting from 60 Oe for simulation (i) and ending at 120 Oe for simulation (iv). Note that the effect of temperature is not taken into account in these simulations, leading to an overestimation of the propagation field values. Depending on the reverse field value, different wall shapes and wall positions can be attained at remanence. So the simulations predict the existence of multiple possible trapped DW positions at remanence. But none of these simulations produces MFM images similar to the observed “bat” shape which our magnetoresistance measurements unambiguously associate with the presence of a trapped DW. Note, however, that the observed “bat” shape may be obtained via a superposition of the different simulated states and of their mirrors. This strongly suggests that the DW is imaged in different positions during the same MFM scan. Hence, the observed “bat” shape likely originates from DW motion induced by the tip. Such motion is not surprising. The effect of MFM tips on micromagnetic configuration was widely studied when the technique was introduced; specifically, DW motion effects induced by MFM tips were observed by Mamin, et al.[13]. In order to confirm this hypothesis we have performed MFM scans in which we vary the scanning history.

Figure 4 shows the results obtained when a DW is present in the free layer for devices with $W= 500, 200, 100$ nm. The smaller notch case ($W= 50$ nm) will be discussed later. Three different scanning procedures have been used; they are named (a), (b) and (c) in the following. Each of them includes two successive scans and the pictures are always recorded during the second scan. The procedure (a) consists in a scan starting from the “bottom” of the device and ending at the “top” of the element immediately followed by a scan performed in the opposite direction (starting from the “top”). During procedure (b) the two successive scans are performed in the same direction from the “bottom” to the “top” part of the device. For procedure (c) the two successive scans are performed from the “top” to the “bottom”. The global trajectory followed by the tip during each procedure is noted by arrows in Fig. 4. The MFM pictures recorded using procedures (a), (b) and (c) are labeled respectively (a), (b) and (c) in Fig. 4. If procedure (a) leads to the observation of the full “bat” shape as expected[14], procedures (b) and (c) generate a discontinuity during the magnetic signal recording. Only the top (bottom) wing of the “bat” is present in images when procedure (b) (procedure (c)) is performed. These three behaviors can be easily understood by taking the DW motion induced by the MFM tip into account. During the first scan of procedure

(a), the tip leaves the DW in a position bordering the top of the notch, and then during the second scan, the tip, moving from top-to-bottom, displaces the DW through the notch. So the DW is imaged in all of the trapping positions induced by the notch, and this leads to the complete “bat” observation. At the end of the first scan of procedure (b), the tip leaves the DW in a position bordering the top of the notch. During the second scan, the MFM tip is unable to image the DW in the bottom position, simply because the domain wall is situated in the top position. So the bottom wing of the “bat” is missing. When the tip approaches close enough to the domain wall, the wall is attracted in an irreversible way, and this leads to the discontinuity in the magnetic signal observed in (b). Then the DW experiences the trapping positions situated on the tip trajectory. This leads to the imaging of the top part of the “bat”. If the two scanning directions of procedure (b) are reversed, we expect that the top wing of the “bat” will be missing, as observed in the images recorded using procedure (c). The same experiments were performed on the smallest notch devices ($W= 50$ nm), but the results obtained were not reproducible from one device to another. We believe that this is due to weaker pinning in the shallower notch depth realized at this dimension.

In conclusion, stripe shaped spin-valves including a sub-micron notch have been fabricated in order to investigate trapped DWs. Combining micromagnetic simulations, transport, and MFM measurements, we have demonstrated that multiple stable states can be created by the notch. Furthermore, the shape and the stability of the wall appears to be dependent on the trapping position. These results should be taken into account when dealing with spin-dependent electronic devices involving trapped DWs because the magneto-electronic properties can change drastically from one stable position to another.

Acknowledgments

We wish to acknowledge M. Hehn and Z. Z. Bandic for helpful discussions.

REFERENCES

- [1] G. Tatara, Y.-W. Zhao, M. Munoz, and N. Garcia, *Phys. rev. Lett.* **83**, 2030 (1999).
- [2] H. D. Chopra and S. Z. Hua, *Phys. Rev. B* **66**, 020403 (2002).
- [3] D. A. Allwood, G. Xiong, M. D. Cooke, C. C. Faulkner, D. Atkinson, N. Vernier, and R. P. Cowburn, *Science* **296**, 2003 (2002).
- [4] N. Vernier, D. A. Allwood, D. Atkinson, M. D. Cooke, and R. P. Cowburn, *cond-mat/0304549* (2003).
- [5] J. Grollier, D. Lacour, V. Cros, A. Hamzic, A. Vaurès, A. Fert, D. Adam, and G. Faini, *J. Appl. Phys.* **92**, 4825 (2002).
- [6] J. Grollier, P. Boulenc, V. Cros, A. Hamzic, A. Vaurès, A. Fert, and G. Faini, *cond-mat/0304312* (2003).
- [7] P. Bruno, *Phys. Rev. Lett.* **83**, 2425 (1999).
- [8] R. D. McMichael, J. Eicke, M. J. Donahue, and D. G. Porter, *J. Appl. Phys.* **87**, 7058 (2000).
- [9] V. A. Molyneux, V. V. Osipov, and E. V. Ponizovskaya, *Phys. Rev. B* **65**, 184425 (2002).
- [10] M. Klaui, C. A. F. Vaz, J. Rothman, J. A. C. Bland, W. Wernsdorfer, G. Faini, and E. Cambril, *Phys. Rev. Lett.* **90**, 097202 (2003).
- [11] T. Ono, H. Miyajima, K. Shigeto, T. Shigeto, and T. Shinjo, *Appl. Phys. Lett.* **72**, 1116 (1998).
- [12] <http://math.nist.gov/oommf>.
- [13] H. J. Mamin, D. Rugar, J. E. Stern, R. E. Fontana, and P. Kasiraj, *Appl. Phys. Lett.* **55**, 318 (1989).
- [14] Indeed, we have used procedure (a) for the acquisition of pictures shown in Fig. 2. Note that (a) is the default procedure currently used in scanned probe microscopy.

FIGURE CAPTIONS

FIG. 1: (a) Schematic representation of the device. (b) Resistance as a function of the applied magnetic field recorded at room temperature for two different field loops ($W=0.5\mu m$). ($-\blacktriangle-$) corresponds to a minor loop in which the magnetization of the free layer is completely switched. During the ($-o-$) loop, a DW is trapped in the notch and then stabilized in zero field.

FIG. 2: Topographic (Topo.) and MFM (MFMA, MFMB) pictures of notches for different geometries. The MFMA pictures correspond to the trapped DW state, while the MFMB images have no DW present.

FIG. 3: Micromagnetic simulations of a trapped DW at remanence for different reverse field values. The absolute values of the reverse fields are respectively equal to 60, 80, 100, 120 Oe for the simulations (i), (ii), (iii) and (iv).

FIG. 4: Schematic representation of the three scanning procedures and MFM pictures of the trapped DW configurations recorded in using these procedures.

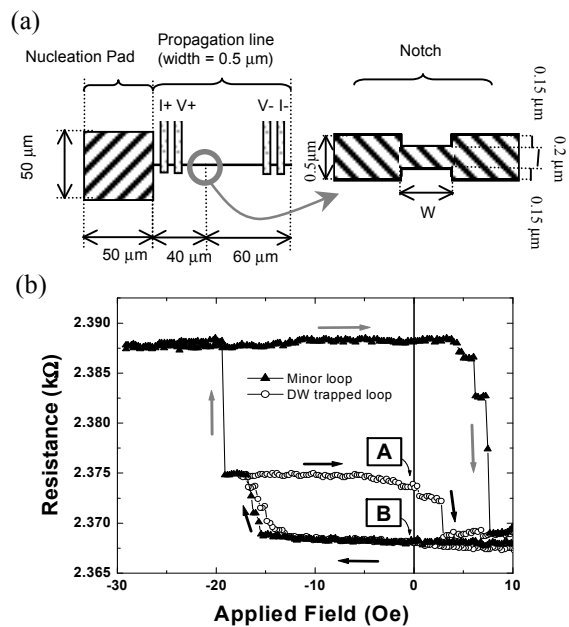


Fig. 1 Lacour et al.

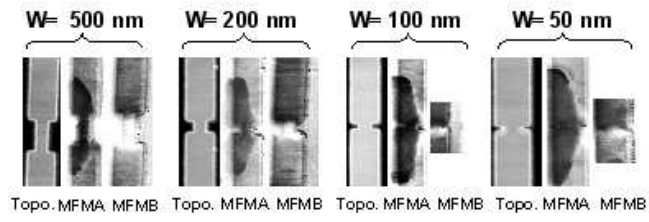


Fig. 2 Lacour et al.

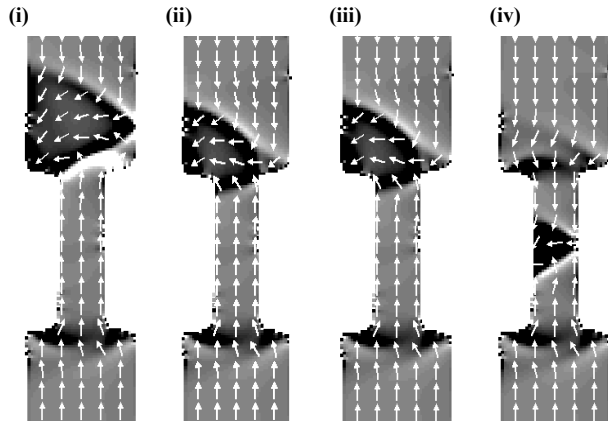


Fig. 3 Lacour et al.

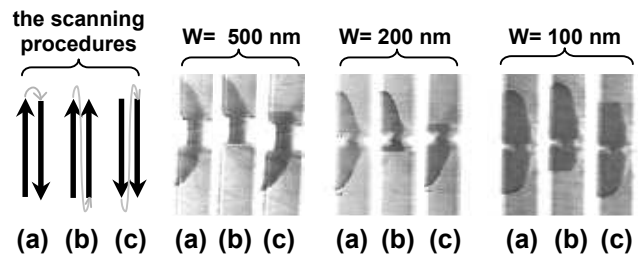


Fig. 4 Lacour et al.